

# DIAGONAL HIERARCHICAL CONSISTENCY LEARNING FOR SEMI-SUPERVISED MEDICAL IMAGE SEGMENTATION

Heejoon Koo

## ABSTRACT

Medical image segmentation, which is essential for many clinical applications, has achieved almost human-level performance via data-driven deep learning techniques. Nevertheless, its performance is predicated upon the costly process of manually annotating a vast amount of medical images. To this end, we propose a novel framework for robust semi-supervised medical image segmentation using diagonal hierarchical consistency learning (DiHC-Net). First, it is composed of multiple sub-models with identical multi-scale architecture but with distinct sub-layers, such as up-sampling and normalisation layers. Second, along with mutual consistency, a novel diagonal hierarchical consistency is enforced between one model’s intermediate and final prediction and other models’ soft pseudo labels in a diagonal hierarchical fashion. Experimental results verify the efficacy of our simple framework, outperforming all previous approaches on public Left Atrium (LA) dataset.

**Index Terms**— Medical Image Segmentation, Semi-supervised Learning, Consistency Regularization, Multi-scale Networks, Entropy Minimization, Uncertainty Estimation

## 1. INTRODUCTION

Medical image segmentation (MIS) involves assigning each pixel in an image to a specific class of anatomical structure, such as organs, tissues and tumours. This task provides valuable information for both computer-aided diagnosis (CAD) and computer-assisted surgery (CAS) in intuitive and efficient manner. Recently, deep learning with U-Net-based architectures [1, 2] has significantly improved MIS. Nonetheless, acquiring a large volume of high-quality annotated medical images remains labour-intensive and time-consuming, necessitating medical experts to manually annotate intricate medical images. To address this issue, many studies have endeavoured on semi-supervised learning that uses a small set of labelled data in conjunction with a large set of unlabelled data [3].

Semi-supervised medical image segmentation (SSMIS) has undergone significant advancements. After a seminal

work by [4], [5] extends it by leveraging deep supervision and hierarchical consistency regularisation. Meanwhile, Li et al. [6] predicts Signed Distance Maps (SDM) [7] as an auxiliary task in an adversarial manner [8] to produce more realistic predictions. Thereafter, [9] introduces dual task consistency between the SDM and segmentation prediction.

Another line of literature [4, 10, 11] introduces uncertainty estimation. Yu et al. [4] introduces uncertainty maps obtained via Monte-Carlo (MC) Dropout to predict with higher confidence in a teacher-student framework. On the other hand, based on findings that uncertainty can be quantified by a statistical discrepancy from multiple model predictions [12], some works design a network comprised of multiple distinct sub-models [10, 11].

During the advancement of SSMIS, computer vision research community has delved into normalisation layers. Instance normalisation [13] is developed for style transfer, while group normalisation [14] has shown great stability on relatively small batch sizes. Albeit these findings, the utilisation of various normalisation layers in SSMIS still remains under-investigated.

Motivated by recent advancements, we introduce a novel framework under the assumption that a network, composed of diversified sub-models, can first fully learn from the scarce labelled data then minimise the disparities in predictions on uncertain regions yielded from both labelled and unlabelled data. Therefore, the main contributions of this paper is three-fold. First, we design the network to be comprised of three identical multi-scale V-Nets [2] with distinct sub-layers, such as up-sampling and normalisation layers to increase intra-model diversity. Second, it is optimised via deep supervision on labelled data and our proposed diagonal hierarchical consistency learning as well as mutual consistency learning [10] on both labelled and unlabelled data. Finally, this simple yet effective framework demonstrates its superiority by surpassing existing baselines on LA dataset [15].

## 2. METHODOLOGIES

### 2.1. Task Formulation

In SSMIS, a set of training data has  $N$  labelled data and  $M$  unlabelled data, where  $N \ll M$ . Then, the small set of labelled data is denoted as  $\mathcal{D}_L = \{x_i^l, y_i\}_{i=1}^N$  and remaining

Email: heejoon.koo.17@alumni.ucl.ac.uk. This work has been submitted to the IEEE for possible publication. Copyright may be transferred without notice, after which this version may no longer be accessible.

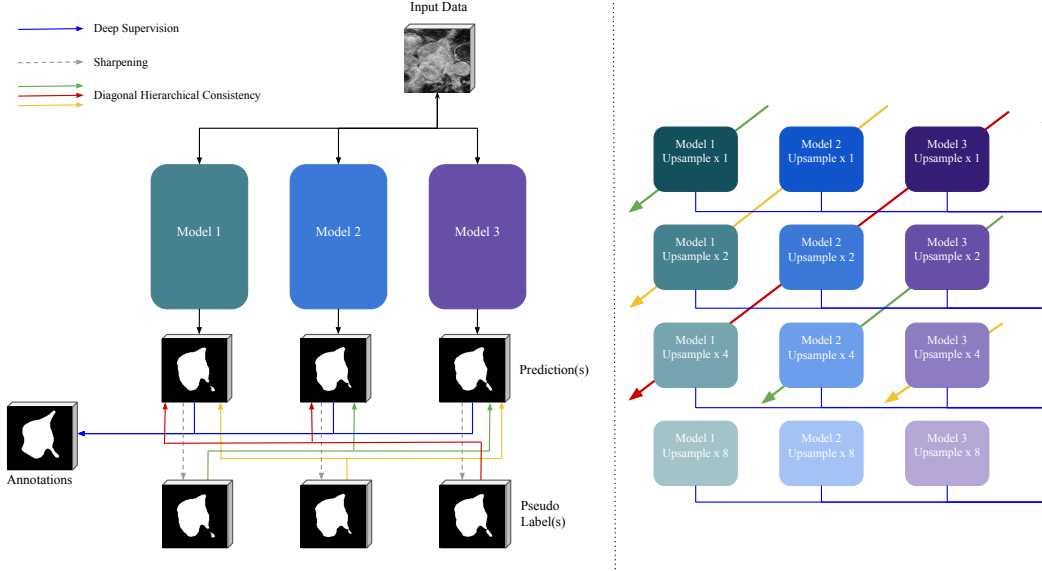


**Fig. 1:** An Overview of Our Proposed Framework, DiHC-Net. The left provides a high-level conceptualisation of the proposed framework, while the right presents a visualisation on both deep-supervision and diagonal hierarchical consistency.

set of unlabelled data as  $\mathcal{D}_U = \{x_i^u\}_{i=1}^M$ , where  $x_i^l$  and  $x_i^u$  denotes the input images and  $y_i$  the corresponding segmentation masks. The objective is to train a model  $f_\theta$ , parameterised with  $\theta$ , using the full data  $\mathcal{D} = \mathcal{D}_L \cup \mathcal{D}_U$  to perform pixel-wise classification correctly.

## 2.2. Diversifying Sub-models

Following the previous works [10, 11], we employ a network with three sub-models having the identical architecture but with a variance in their sub-layers. Specifically, we use group normalisation [14] and linear interpolation for the first sub-model’s normalisation and up-sampling, respectively. The second sub-model configures with transposed convolution and batch normalisation [16] and the third model adopts nearest interpolation and instance normalisation [13].

Also, we extend our sub-models to have multi-scale architecture to produce intermediate representations from each block in their decoding stage. On the labelled data, the network learns scarce supervisory signal effectively by minimising the differences between up-sampled intermediate predictions and ground truths in each sub-models. This supervised segmentation loss is mathematically formulated as:

$$\mathcal{L}_{sup} = \sum_{m=1}^M \sum_{s=1}^S \mathcal{L}_{dice}(f_m^s(x_i^l), y_i), \quad (1)$$

where  $\mathcal{L}_{dice}$  represent dice loss,  $f_m^s(\cdot)$  denotes the predicted results from at scale  $s$  of  $m$ -th model. Both  $s$  and  $m$  are integers, ranging from 1 to 3 and 4, respectively.

## 2.3. Diagonal Hierarchical Consistency Learning

Boosting diversity amongst sub-models leads to increased inconsistent predictions especially in challenging regions. These uncertainties can be mitigated effectively by employing pseudo labels to minimise entropy across the models. To this end, we partition the consistency loss term into two distinct loss terms: conventional mutual consistency loss [10] and our novel diagonal hierarchical consistency loss. It is applied to both labelled and unlabelled data.

First, following the previous studies [10, 11], we enforce intra-model consistency between the soft pseudo labels converted from one sub-model’s final prediction and others’ final predictions. The sharpening function [17] is utilised to define the pseudo label as follows:

$$S^{M_n} = \text{sharpening}(p^{M_n}), \quad (2)$$

$$\text{where sharpening} = \frac{p^{1/T}}{p^{1/T} + (1-p)^{(1/T)}}.$$

Here,  $S$  and  $p$  represent the pseudo label and prediction, respectively, while  $M_n$  denotes the  $n$ -th model. The hyper-parameter  $T$  serves to control entropy; a lower  $T$  promotes low-entropy predictions. Then, with  $\alpha_k$  as the coefficient for the  $k$ -th block at the decoding stage, the formulation of the mutual consistency loss using mean squared error (MSE) is:

$$\mathcal{L}_{MC} = \sum_{i,j=1 \& i \neq j}^n \alpha_1 \text{MSE}(S_i^{M_i}, p_j^{M_j}). \quad (3)$$

Next, our novel diagonal hierarchical consistency minimises the difference between one sub-model’s pseudo labels

converted from its final representation and others’ intermediate representations. Let the coordinate of representation as ( $m$ -th model,  $s$ -th representation). Then, the representation from the last decoding block of the first model is (1, 1). Similarly, the representation from the first decoding block of the third model is (3, 4). We do not perform the self-constraint between the pseudo label and the first decoder block from the same model due to empirical harmful effects. Thus, the regarding loss is formulated as:

$$\begin{aligned} \mathcal{L}_{DHC} = & \alpha_2 \text{MSE}(S_1^{M_1}, p_2^{M_3}) + \alpha_3 \text{MSE}(S_1^{M_1}, p_3^{M_2}) \\ & + \alpha_2 \text{MSE}(S_2^{M_2}, p_2^{M_1}) + \alpha_3 \text{MSE}(S_2^{M_2}, p_3^{M_3}) \quad (4) \\ & + \alpha_2 \text{MSE}(S_3^{M_3}, p_2^{M_2}) + \alpha_3 \text{MSE}(S_3^{M_3}, p_3^{M_1}). \end{aligned}$$

Therefore, the network is optimised via a weighted sum of supervised loss  $\mathcal{L}_{sup}$  and consistency loss  $\mathcal{L}_{CST}$ .

$$\begin{aligned} \mathcal{L}_{TOTAL} = & \lambda_{SUP} \mathcal{L}_{sup} + \lambda_{CST} \mathcal{L}_{CST}, \quad (5) \\ \text{where } \mathcal{L}_{CST} = & \mathcal{L}_{MC} + \mathcal{L}_{DHC}, \end{aligned}$$

where  $\lambda_{SUP}$  denotes a hyper-parameter for the supervised loss and  $\lambda_{CST}$  is the coefficient for the consistency loss, which is a time-dependent Gaussian warming-up function that balances between two loss terms. It is formalised as  $\lambda(t) = 0.1 * \exp(-5(1 - t/t_{max}))$  where  $t$  and  $t_{max}$  are present training step and the maximum step, respectively. It addresses the potential issue of consistency loss term that may harm the learning in the early stage.

### 3. EXPERIMENTAL SETTING

#### 3.1. Dataset

To validate the effectiveness of our approach, we conduct experiments on publicly available Left Atrium (LA) dataset. It provides 100 3D MRI scans and corresponding segmentation masks. All scans are cropped centring on the heart region, with an intensity normalisation to have zero mean and unit variance. As test set annotations are publicly unavailable, the training set is divided into two subsets, with 80 scans for training and 20 scans for evaluation.

#### 3.2. Implementation Details

For training scheme, we follow the previous works [4, 6, 10]. First, we perform two settings: training with 10% or 20% labelled data and the remaining unlabelled data. Then, we apply data augmentation by randomly rotating and flipping with 90, 180, and 270 degrees along the axial plane. Afterwards, input sub-volumes of  $112 \times 112 \times 80$  are extracted via cropping.

For the hyper-parameter setting, a batch size is set to 4 so that each batch contains two labelled data and two unlabelled data. Soft pseudo labels are generated using a sharpening function with a fixed temperature  $T$  of 0.1. The network is updated using an SGD optimiser for 15k iterations, with

an initial learning rate of  $1e-2$  decayed by 0.1 for every 2.5k iterations and a weight decay factor of  $1e-4$ . We use three intermediate representations and coefficients for each consistency loss are determined as  $\alpha_1 = 1.0$ ,  $\alpha_2 = 0.75$ , and  $\alpha_3 = 0.5$ . We set them to gradually decrease, since intermediate blocks should be softly regularised due to their tendency to produce relatively incomplete outputs. Also, we set hyper-parameter for supervised loss  $\lambda_{sup}$  as 1. Finally, instead of averaging outputs, the results only from the first model are used.

For the evaluation, a sliding window of  $112 \times 112 \times 80$  with a stride of  $18 \times 18 \times 4$  is employed to extract and recombine patches. For fair comparison, we do not apply any post-processing module, such as non-maximum suppression.

#### 3.3. Evaluation Metrics

We measure the quantitative performance using four widely used metrics: Dice, Jaccard, 95HD (95% Hausdorff Distance), and ASD (Average Surface Distance). The first two metrics assess the interior segmentation predictions, while the last two assess the contour predictions.

## 4. EXPERIMENTAL RESULTS

#### 4.1. Performance Comparison

Table 1 presents the quantitative results of our proposed method and other strong baselines, including UA-MT [4], SASS [6], DTC [9], MC-Net+ [10] and CC-Net [11]. As shown in Table 1, our DiHC-Net outperforms all baselines by a significant margin in both training settings. Specifically, our method outperforms the current state-of-the-art method, MC-Net+ [10], by 1.46% and 0.87% in Dice score when trained with 10% and 20% labelled data, respectively. Furthermore, our method achieves a 95HD score that is 0.87mm and 1.46mm smaller than that of MC-Net+, demonstrating the robustness of our approach in contour segmentation as well. Fig. 2 visually highlights the effectiveness and robustness of our approach. Our framework is more stable to false positives and produces more natural contours than shape-constraint methods [6, 9] (first row). Moreover, ours predicts the organ region that other methods cannot predict and sound to true negatives (second row).

#### 4.2. Ablation Studies

We also conduct ablation studies to discern each proposed module’s impact on the overall performance. We present the regarding results to Table 2. Our design components are abbreviated as: 1) Intra-Model Diversity (IMD), 2) Multi-scale Network (MS), and 3) diagonal Hierarchical Consistency (DiHC). The model does not incorporate any components is equivalent to MC-Net+ [10].

First, applying IMD does not consistently result in overall performance enhancement, particularly when comparing

Method	# Scans used		Metrics			
	Labelled	Unlabelled	Dice(%) $\uparrow$	Jaccard(%) $\uparrow$	95HD(voxel) $\downarrow$	ASD(voxel) $\downarrow$
UA-MT [4]	8 (10%)	72 (90%)	84.25	73.48	13.84	3.36
SASS [6]			86.81	76.92	12.54	3.94
DTC [9]			87.51	78.17	8.23	2.36
MC-Net+ [10]			88.96	80.25	7.93	1.86
CC-Net [11]			89.82	81.60	7.03	1.8
<b>Ours (DiHC-Net)</b>			<b>90.42</b>	<b>82.58</b>	<b>6.52</b>	<b>1.54</b>
UA-MT [4]	16 (20%)	64 (80%)	88.88	80.21	7.32	2.26
SASS [6]			89.27	80.82	3.13	8.83
DTC [9]			89.42	80.98	7.32	2.1
MC-Net+ [10]			91.07	83.67	5.84	1.67
CC-Net [11]			91.27	84.02	5.75	1.54
<b>Ours (DiHC-Net)</b>			<b>91.94</b>	<b>85.13</b>	<b>5.03</b>	<b>1.35</b>

**Table 1:** A Quantitative Performance Comparison on the LA Dataset.

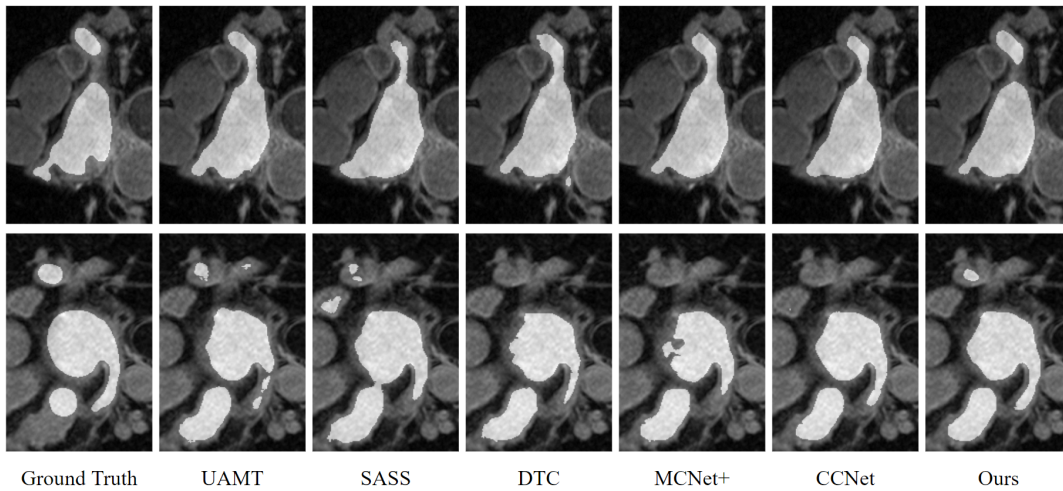


**Fig. 2:** 2D Visualisation of Ground Truth and Predictions of Our DiHC-Net and Other Baselines on LA Dataset. The first row is acquired when trained with 10% labelled data and the second row with 20% labelled data.

contour-related metrics, 95HD and ASD. This suggests that merely enhancing the diversity in the configurations of sub-models complicates the convergence process. However, the integration of MS and IMD results in performance improvement, as they fully leverage supervisory signals. Furthermore, integrating DHC with the other components leads to significant gains across all metrics and both training settings, verifying our initial hypothesis.

## 5. CONCLUSION

In this paper, we present a simple but effective SSMIS framework. Its network is composed of three sub-models with the same multi-scale architecture but distinct sub-layers to increase the intra-model diversity. By employing deep supervision, the sub-models first learn the limited labelled data. Next, they collaborate by minimising disparity on challenging regions by comparing soft pseudo labels from one’s final

# Scans Used		Designs			Metrics	
Labelled	Unlabelled	IMD	MS	DiHC	Dice(%) $\uparrow$	95HD(voxel) $\downarrow$
8 (10%)	72 (90%)				88.96	7.93
		✓			89.53	10.17
		✓	✓		90.13	8.76
		✓	✓	✓	<b>90.42</b>	<b>6.52</b>
16 (20%)	64 (80%)				91.07	5.84
		✓			91.1	6.8
		✓	✓		91.72	7.06
		✓	✓	✓	<b>91.94</b>	<b>5.03</b>

**Table 2:** Ablation Studies on the LA Dataset.

predictions and others’ intermediate and final outcomes via conventional mutual consistency and our diagonal hierarchical consistency on both labelled and unlabelled data. Experimental results demonstrate the superiority and robustness of our DiHC-Net.

**Compliance with Ethical Standards** This research was conducted retrospectively using LA dataset [15] (open access human subject data), thus ethical approval was not required.

## 6. REFERENCES

- [1] Olaf Ronneberger, Philipp Fischer, and Thomas Brox, “U-net: Convolutional networks for biomedical image segmentation,” in *Medical Image Computing and Computer-Assisted Intervention—MICCAI 2015: 18th International Conference, Munich, Germany, October 5-9, 2015, Proceedings, Part III* 18. Springer, 2015, pp. 234–241.
- [2] Fausto Milletari, Nassir Navab, and Seyed-Ahmad Ahmadi, “V-net: Fully convolutional neural networks for volumetric medical image segmentation,” in *2016 fourth international conference on 3D vision (3DV)*. Ieee, 2016, pp. 565–571.
- [3] Rushi Jiao, Yichi Zhang, Le Ding, Rong Cai, and Jicong Zhang, “Learning with limited annotations: a survey on deep semi-supervised learning for medical image segmentation,” *arXiv preprint arXiv:2207.14191*, 2022.
- [4] Lequan Yu, Shujun Wang, Xiaomeng Li, Chi-Wing Fu, and Pheng-Ann Heng, “Uncertainty-aware self-ensembling model for semi-supervised 3d left atrium segmentation,” in *Medical Image Computing and Computer Assisted Intervention—MICCAI 2019: 22nd International Conference, Shenzhen, China, October 13–17, 2019, Proceedings, Part II* 22. Springer, 2019, pp. 605–613.
- [5] Shumeng Li, Ziyuan Zhao, Kaixin Xu, Zeng Zeng, and Cuntai Guan, “Hierarchical consistency regularized mean teacher for semi-supervised 3d left atrium segmentation,” in *2021 43rd Annual International Conference of the IEEE Engineering in Medicine & Biology Society (EMBC)*. IEEE, 2021, pp. 3395–3398.
- [6] Shuailin Li, Chuyu Zhang, and Xuming He, “Shape-aware semi-supervised 3d semantic segmentation for medical images,” in *Medical Image Computing and Computer Assisted Intervention—MICCAI 2020: 23rd International Conference, Lima, Peru, October 4–8, 2020, Proceedings, Part I* 23. Springer, 2020, pp. 552–561.
- [7] Jun Ma, Zhan Wei, Yiwen Zhang, Yixin Wang, Rongfei Lv, Cheng Zhu, Chen Gaoxiang, Jianan Liu, Chao Peng, Lei Wang, et al., “How distance transform maps boost segmentation cnns: an empirical study,” in *Medical Imaging with Deep Learning*. PMLR, 2020, pp. 479–492.
- [8] IJ Goodfellow, J Pouget-Abadie, M Mirza, B Xu, D Warde-Farley, S Ozair, and Y Bengio, “Generative adversarial networks, 1–9,” *arXiv preprint arXiv:1406.2661*, 2014.
- [9] Yichi Zhang and Jicong Zhang, “Dual-task mutual learning for semi-supervised medical image segmentation,” in *Pattern Recognition and Computer Vision: 4th Chinese Conference, PRCV 2021, Beijing, China, October 29–November 1, 2021, Proceedings, Part III* 4. Springer, 2021, pp. 548–559.
- [10] Yicheng Wu, Zongyuan Ge, Donghao Zhang, Minfeng Xu, Lei Zhang, Yong Xia, and Jianfei Cai, “Mutual consistency learning for semi-supervised medical image segmentation,” *Medical Image Analysis*, vol. 81, pp. 102530, 2022.
- [11] Hejun Huang, Zuguo Chen, Chaoyang Chen, Ming Lu, and Ying Zou, “Complementary consistency semi-supervised learning for 3d left atrial image segmentation,” *Computers in Biology and Medicine*, vol. 165, pp. 107368, 2023.
- [12] Balaji Lakshminarayanan, Alexander Pritzel, and Charles Blundell, “Simple and scalable predictive uncertainty estimation using deep ensembles,” *Advances in neural information processing systems*, vol. 30, 2017.
- [13] Dmitry Ulyanov, Andrea Vedaldi, and Victor Lempitsky, “Instance normalization: The missing ingredient for fast stylization,” *arXiv preprint arXiv:1607.08022*, 2016.
- [14] Yuxin Wu and Kaiming He, “Group normalization,” in *Proceedings of the European conference on computer vision (ECCV)*, 2018, pp. 3–19.
- [15] Zhaohan Xiong, Qing Xia, Zhiqiang Hu, Ning Huang, Cheng Bian, Yefeng Zheng, Sulaiman Vesal, Nishant Ravikumar, Andreas Maier, Xin Yang, et al., “A global benchmark of algorithms for segmenting the left atrium from late gadolinium-enhanced cardiac magnetic resonance imaging,” *Medical image analysis*, vol. 67, pp. 101832, 2021.
- [16] Sergey Ioffe and Christian Szegedy, “Batch normalization: Accelerating deep network training by reducing internal covariate shift,” in *International conference on machine learning*. pmlr, 2015, pp. 448–456.
- [17] Qizhe Xie, Zihang Dai, Eduard Hovy, Thang Luong, and Quoc Le, “Unsupervised data augmentation for consistency training,” *Advances in neural information processing systems*, vol. 33, pp. 6256–6268, 2020.